The Pre-Breakdown Phenomena in Atmospheric Air Gaps under the Impulse Voltage

By

Hiromu Isa,* and Muneaki Hayashi*

(Received September 28, 1976)

Abstract

Pre-breakdown phenomena against impulse voltage are observed, where rod-to-plane electrodes are used, and the gap length is 3~20 cm. Streamers are observed by an oscillograph, a still camera acompanied with chopped voltage and a photo-multiplier. As the result of this investigation, for a positive and a negative polarity, the number of charged particles, the field intensities of primary and secondary streamers were obtained experimentally. Furthermore, the difference between a positive and a negative polarity was considered.

1. Introduction

In such a non-uniform field as the rod-to-plane gap, the phenomena from a streamer occurrence to a complete breakdown are very complicated. It is reported that the breakdown for a short gap of $\delta < 10$ cm occurs in the order of a primary streamer, a secondary streamer and an arc,[1]−[3] while for a gap of $\delta > 10$cm, the order is a streamer, a leader and an arc.[4]−[6] In this study, the pre-breakdown phenomena for δ in the range of 3~20 cm were observed by means of a still photograph, current and light pulse waves. The purpose is for the investigation of the characteristics of a primary and a secondary streamer as well as the study of their development mechanism.

2. Experimental Apparatus and Measuring Methods

Fig. 1 shows the schematic diagram of the experimental arrangement. The impulse voltage generator has a resultant capacitance of $0.05\,\mu$F, a damping resistor 80 Ω and a nominal voltage 280kV. The output voltage is $\pm (1 \times 40)\,\mu$s standard light-

---

* Department of Electrical Engineering

ning impulse, and the wave front steepness can be adjusted by the resistor R_1 and the condencer C_1. By inserting the gap at the point *(Fig. 1), a steep impulse voltage $(T_f=20\text{ns})$ can be obtained. Through the delay circuit, the impulse voltage triggers gap G_1 and the applied main voltage across the test gap can be chopped at any instant, if necessary.
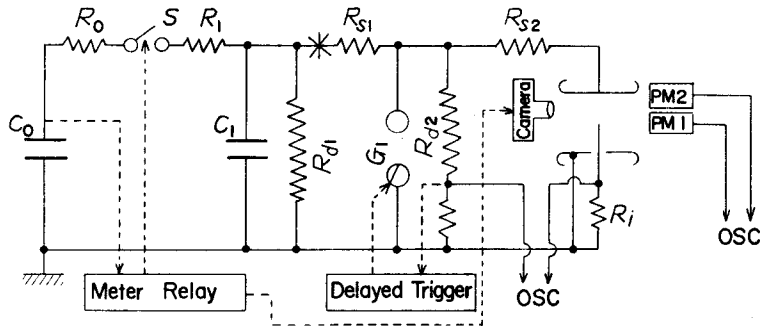
C_0 =0.05 μF, C_1=1100 pF, R_0=80Ω, R_1=250Ω,
R_{S1} =250Ω, R_{S2} =45Ω, R_{d1}=1 kΩ, R_{d2}=10 kΩ,
R_i =75Ω, G_1: Gap for voltage chopping

Fig. 1. Arrangement of experimental apparatus.

The test gap electrodes consist of a hemispherically-capped cylindrical rod and a plane electrode which are made of brass. The radius of curvature of the rod tip (ρ) are 2, 3, 5mm, and a 2mm rod was mainly used. The plane electrode is a disc plate with a 25 cm diameter and has a round edge with a 1.5 cm curvature. The commonly used gap arrangement is shown in Fig. 2(a), but because it has the demerit of being easily affected by a charging current and noises during the measurement of the current, a guard electrode with the same shape as the plane electrode is used as shown in Fig. 2(b). Only in special cases was the arrangement shown in (a) used. In this report, (a) and (b) arrangements are called normal and reversed, respectively. In both arrangements, the polarity of the applied voltage is determined by the relative potential of rod to plane.

The applied voltage and the current wave form, across the output of the divider resistor R_{d2} and the current measuring resistor (so called shunt resistor) R_i were observed by using an oscilloscope (Iwasaki SS550-A1, or Tektronics type 507). The figure of the discharge phenomenon across the test gap was taken by using a still-photo camera (Cannon F1, lens f=50 mm, F=1.4 or f=100 mm, F=2.8). At the same time, by means of employing 2 sets of photomultipliers, PM1 and PM2, the light pulse caused by the discharge could be measured. Both PM1 and PM2 have
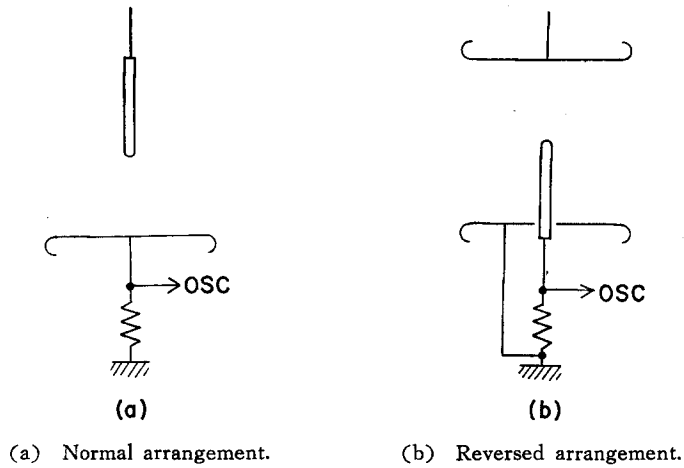
(a)   Normal arrangement.   (b)   Reversed arrangement.

Fig 2. Gap arrangement.

a slit (the s it area on the gap axis is 0.8 mm×60 mm), and they could be adjusted on any position along the gap axis. The positions are expressed by the distance from the rod tip and are denoted by x. The output pulses of PM1 and PM2 were observed by using a Tektronics type 556 oscilloscope (2 beams). Still photographs and wave forms on an oscilloscope were recorded on Kodak Tri-X film. Table 1 shows the list of experimental equipment used here.

Table 1. List of experimental equipments.

equipments	type, ability, etc.	function
impulse generator	0.2μF×4-stages, nominal voltage 280kV, 1.96kJ	voltage supply
damper register	330 Ω	
wave front compensator	1100pF ceramic capacitor	
main circuit resistor	Tama Electric Type PSO 1kΩ	
potential divider	〃 Type PSO 10kΩ	
current detector	Rikenohm type S, 75Ω	
oscilloscope	Iwasaki SS550A1 or Tektronics Type 507	current measurement
〃	Tektronics Type 556	applied voltage and light pulse measurement
photomultiplier	Toshiba 7696×2	light pulse measurement
camera	Cannon F1×2, Asahi SP×1	still photo, oscillogram recording
〃	Asahi SL×2	optics for light pulse measurement
photo-film	Kodak Tri-X	still photo, oscillogram recording

3. Characteristics of the Primary Streamer

3.1 Positive Streamer

⟨3.1.1⟩ The Propagating Velocity and its Distance

When an impulse voltage is applied to the rod-to-plane gap, a primary streamer (abbreviated as PS in the following) develops first under a normal gap arrangement, where ρ (radius of the rod tip) = 2 mm and δ (gap length) = 10 cm.[1)-6)9)] The streamer propagating distance l vs. time t for the applied voltage V_s as the parameter is shown in Fig. 3. The gradient of the curve in Fig. 3 indicates the propagating velocity of the PS. When the applied voltage is low, the velocity decreases as the
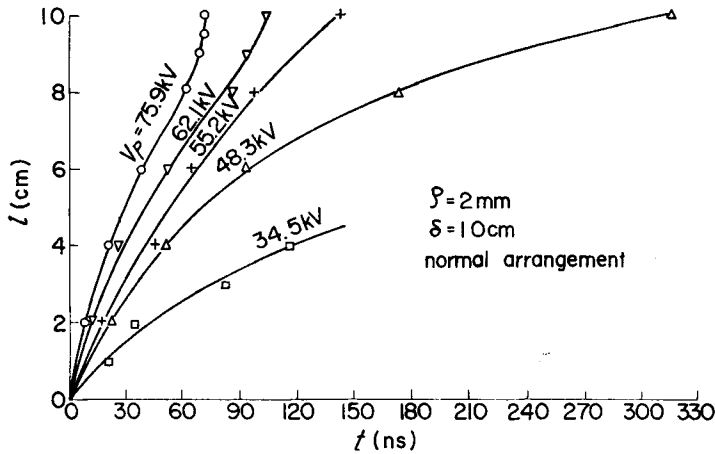
Fig. 3. t-l characteristics for psitive PS.

Table 2. Average developing velocity of positive PS.

investigator	velocity (cm/s)
Hudson, Loeb[1)]	$2\times10^{7}\sim6\times10^{8}$
Dawson[2)]	$2.0\times10^{7}\sim6.3\times10^{7}$
Acker, Penney[3)]	$2.9\times10^{7}\sim1.9\times10^{8}$
Nasser, Loeb[10)]	1.2×10^{8}
Kritzinger[11)]	$2\times10^{7}\sim1\times10^{8}$
Kritzinger[12)]	$1.5\times10^{7}\sim1\times10^{8}$
Stekol'nikov, Shkilev[13)]	$5\times10^{7}\sim1\times10^{8}$
Suzuki[14)]	$9\times10^{6}\sim1.8\times10^{8}$
authors	$3.2\times10^{7}\sim1.4\times10^{8}$

propagating distance increases. But as the applied voltage becomes high, the velocity decreases in the mid gap and increases again near the cathode. The average velocity v_{av} of the PS can be expressed by δ/T_1, where T_1 equals the PS travelling time across the gap. From Fig. 3, it is deduced that the higher the applied voltage, the greater the velocity will be. Further, v_{av} is found to be $3.2\times10^7\sim1.4\times10^8$ cm/s which coincides approximately with the results obtained by other researchers (Table 2).[1]—[3] [10]—[14]
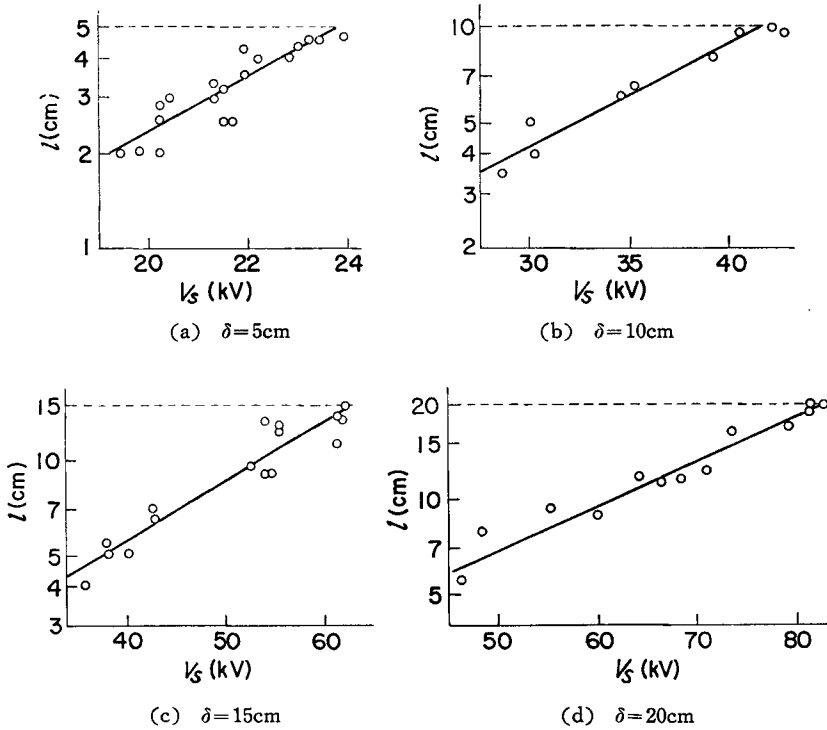

Fig. 4. V_s-l characteristics for positive PS. $\rho=2$mm, normal arrangement.

The voltage at the instance of the PS occurrence V_s vs. the PS length l was obtained as shown in Fig. 4. From this result, it is deduced that l varies exponentially with V_s. Assuming a constant field in the longitudinal direction of the PS,[16] the average field intensity can be calculated. For $\delta=5$, 10, 15, 20 cm, the average fields are 4.8, 4.2, 4.2 and 4.1 kV/cm respectively. These values are slightly less than the flashover field intensity for the long gap.[17]

⟨3.1.2⟩ **Electrical Current and Charge**

Fig. 5 shows the peak value of the current pulse (i_s) vs. the voltage at the instance of the PS occurrence V_s. The curve shows an exponential variation[13][14]
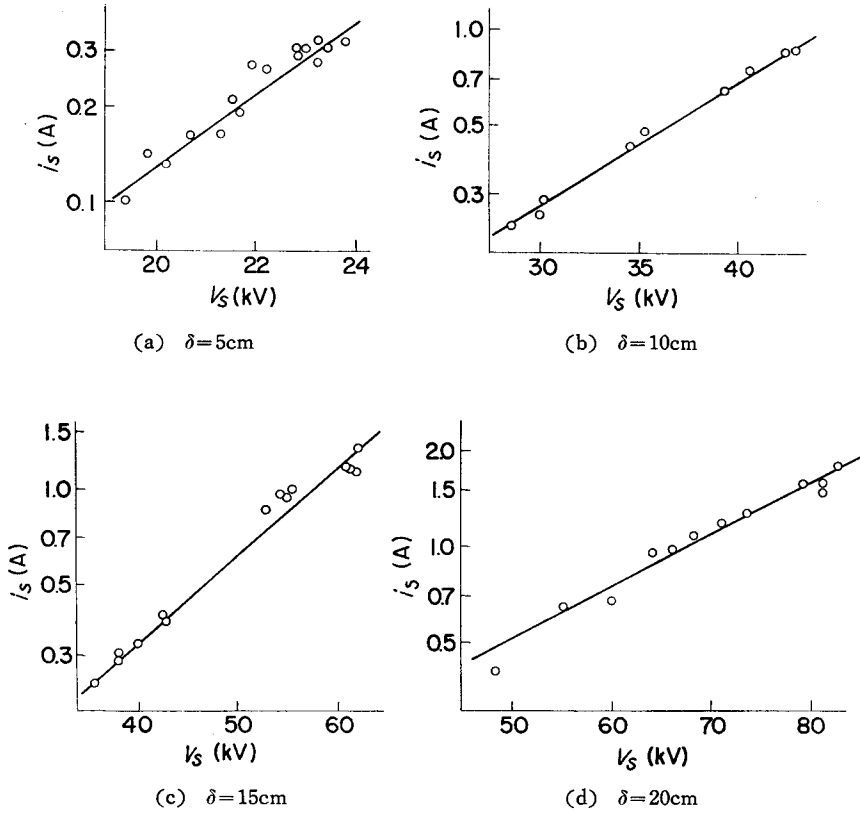
Fig. 5. $V_s - i_s$ characteristics for positive PS. $\rho = 2\text{mm}$, normal arrangement.

similar to that of the $l - V_s$ curves. When the applied voltage is lower than the PS bridgeover level for the gap, the current which flows through the gap can be expressed by the following equation

$$i_s = \int_0^l enSv \frac{E}{V} \, dl \qquad\qquad (1)^{15)}$$

where, e: electrical charge of electron, n: density of electron number, v: drift velocity of electron, E: electric field intensity, V: applied voltage, S: cross section area of PS.

Assuming the field within the PS channel to be constant, v becomes constant and

$$i_s = ev \frac{E}{V} \int_0^l nS \, dl \qquad\qquad (2)$$

From Fig. 4 and 5, the relationship between l and i_s can be established, and is shown in Fig. 6. From these results, it is deduced that i_s increases proportionally with l. Although the increase is slightly larger than the direct proportional rate, ex-

cepting the case of $\delta=15$ cm, the values can be kept within a range of $\pm$ 20% even if direct proportionality is assumed. According to Eq. (2), the i_s increase due to the V_s increase is caused by both an increase of the electron numbers nS per cm in the PS length and the PS length l. The reason why the curve in Fig. 6 deviates from the straight line is probably due to the nS increase. However, in this paper, nS is assumed to be constant, according to Loeb.[16]
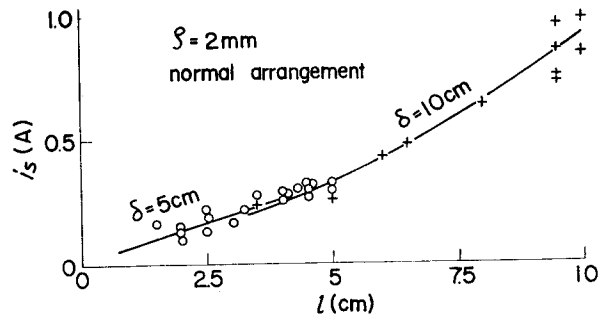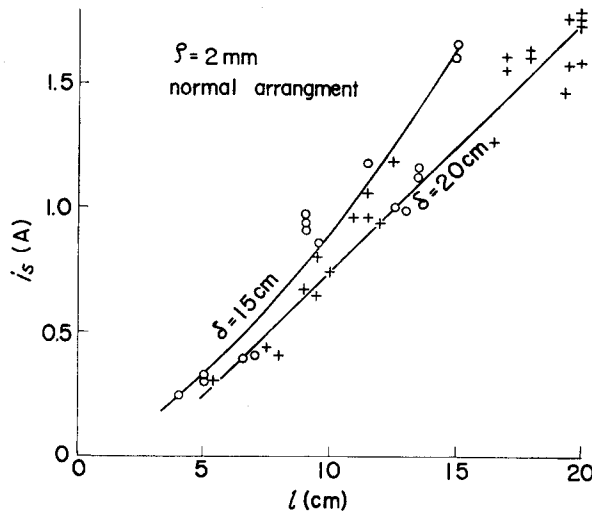
Fig. 6. l–i_s characteristics for positive PS.

By integrating the current flow over the total time of pre-discharge, the total discharge amount caused by the PS can be obtained. Further, the current wave form, the total amount of discharge and the charge quantity per cm length of the streamer were measured for the various gap lengths δ (5~20 cm) subiected to the applied voltage by which the PS can just bridge the gap. The results obtained are

Table 3. Physical quantities when positive PS just bridges over the gap.

δ(cm) Physical quantities	5	10	15	20
total amount of discharge (C)	3.2×10^{-8}	5.6×10^{-8}	8.0×10^{-8}	1.0×10^{-7}
charge per cm (C/cm)	6.3×10^{-9}	5.6×10^{-9}	5.3×10^{-9}	5.2×10^{-9}
total number of electrons	2.0×10^{11}	3.5×10^{11}	5.0×10^{11}	6.5×10^{11}
electrons per cm	3.9×10^{10}	3.5×10^{10}	3.3×10^{10}	3.3×10^{10}
electron density (cm^{-3})	$1.3\sim5.0\times10^{12}$	$1.1\sim4.5\times10^{12}$	$1.1\sim4.2\times10^{12}$	$1.0\sim4.1\times10^{12}$
total energy (J)	7.7×10^{-4}	2.4×10^{-3}	4.9×10^{-3}	8.5×10^{-3}
energy per cm (J/cm)	1.5×10^{-4}	2.4×10^{-4}	3.3×10^{-4}	4.2×10^{-4}
voltage at PS occurrence (kV)	25	42	62	81
current peak (A)	0.28	0.79	1.2	1.5

shown in Table 3. The total charge increases with δ but the charge per cm remains constant. These values expressed in terms of an electron number are shown in columns 3 and 4 of Table 3. Assuming the diameter of the PS to be $1\sim2$ mm, the density of the charged particle is obtained as shown in column 5. During the PS development, if the applied voltage is kept constant, the total energy which is supplied into the gap space and the energy per cm length of the streamer are obtained as shown in columns 6 and 7. Based on these energy data, it is concluded that the energy increases with δ. Further, according to Kritzinger,[12] the space charge generated during the streamer propagation is 3×10^{-9} C per streamer. As there exist
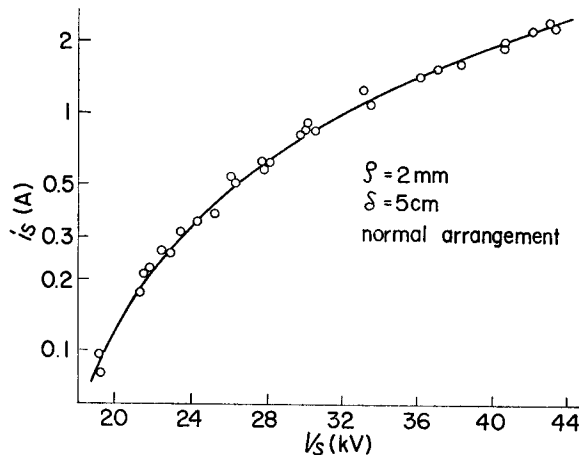

Fig. 7. V_s–i_s characteristics for positive PS under wide range of V_s. $\rho=2$mm, $\delta=5$cm, normal arrangement.

several dozens of streamers, a rough calculation shows that Kritzinger's value agrees with that in Table 3. In Fig. 5, the exponential relationship between i_s and V_s has roughly been established, but the i_s—V_s characteristics in the range from the inception voltage of the PS to the flashover show a saturation tendency as shown in Fig. 7.

3.2 Negative Streamer

Contrary to the positive polarity case, when a negative impulse is applied to the gap, owing to the PS occurrence in the midst of the voltage wave front, a result such as that in Fig. 3 is hard to obtain. However, the measurement of the average velocity of the PS across the gap is feasible. For instance, for $\delta=5$ cm, v_{av} has a value between $5.0\times10^7 \sim 2.5\times10^8$cm/s which is about equal to those obtained by other researchers (Table 4).[4)18)—20)]

Table 4. Average developing velocity of negative PS.

investigator	velocity (cm/s)
Suzuki[18)	$2\sim7\times10^7$, $2\sim12\times10^6$
Park, Cones[4)	5×10^3
Nasser[19)	$2.2\sim14\times10^8$
Tsuneyasu et al.[20)	$1.3\sim1.8\times10^7$
authors	$5\sim25\times10^7$

The experimental results of the PS length l vs. the occurrence voltage V_s and of the current peak value i_s vs. V_s are shown in Fig. 8 and 9 respectively. In these
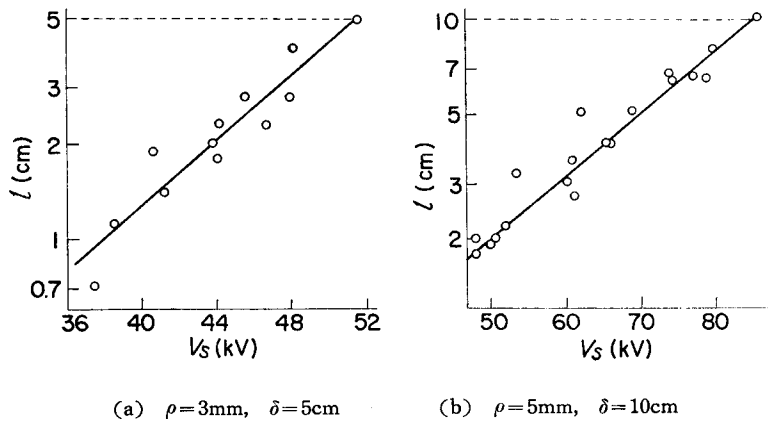

(a) $\rho=3$mm, $\delta=5$cm   (b) $\rho=5$mm, $\delta=10$cm

Fig. 8. V_s-l characteristics for negative PS. Normal arrangement.

(a) $\rho = 3$mm, $\delta = 5$cm   (b) $\rho = 5$mm, $\delta = 10$cm
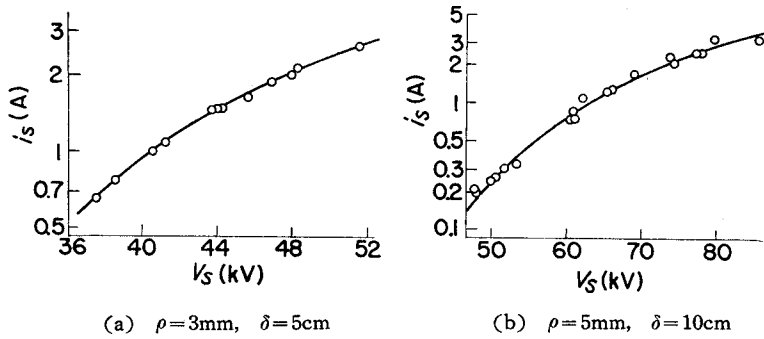
Fig. 9. V_s-i_s characteristics for negative PS. Normal arrangement.

cases, the electrodes of $\rho = 3$ mm ($\delta = 5$ cm) and $\rho = 5$ mm ($\delta = 10$ cm) were used to obtain data about the wide range of V_s. It is deduced from these results that V_s shifts considerablly towards a higher value compared to the positive polarity case. Such a difference is possibly caused not only by the different value of ρ but the difference in the development mechanism between the positive and negative stream-ers. From Fig. 8 and 9, the characteristic of i_s vs. l can be established and it is almost linear as shown in Fig. 10. Similar to the positive streamer, the average field intensities observed in the negative PS based on V_s where $\delta = 5$, 10 cm, are 10.3 and 8.6 kV/cm respectively, and they are almost twice as much as that of the positive PS.
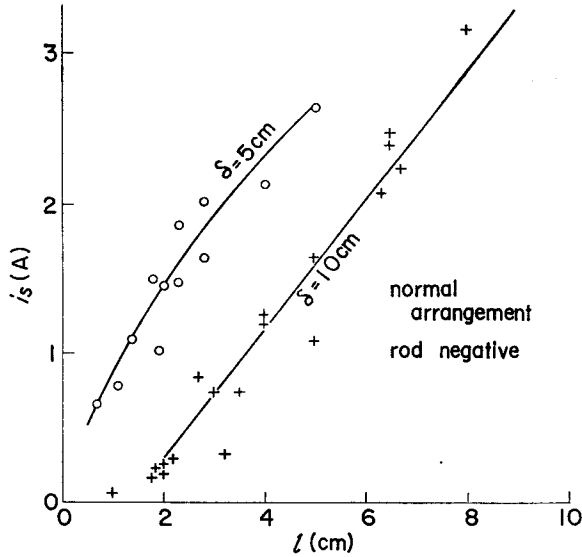

Fig. 10. $l-i_s$ characteristics for negative PS.

The discharge quantity caused by the negative PS and the input energy to the PS etc. where $l=\delta$ are as shown in Table 5. Compared with that of the positive PS, the increase of the discharge quantity is about 3 times, and that of the input energy is 6~7 times. Hence, for the negative PS development, a stronger electric field and a larger energy tha in the case of a positive PS are necessary, and it would be one of the causes of polarity effect in various characteristics of discharge. However, the charge and energy in each unit length vs. δ have a tendency similar to that of the positive polarity.

Table 5. Physical quantities when negative PS just bridges over the gap.

δ (cm) / Physical quantities	5	10
total amount of discharge (C)	1.0×10^{-7}	1.6×10^{-7}
charge per cm (C/cm)	2.1×10^{-8}	1.6×10^{-8}
total number of electrons	6.5×10^{11}	9.8×10^{11}
electrons per cm	1.3×10^{11}	9.8×10^{10}
electron density (cm^{-3})	$4.1 \sim 17 \times 10^{12}$	$3.1 \sim 13 \times 10^{12}$
total energy (J)	5.4×10^{-3}	1.3×10^{-2}
energy per cm (J/cm)	1.1×10^{-3}	1.3×10^{-3}
voltage at PS occurrence (kV)	52	86
current peak (A)	2.6	3.2

3.3 The Formation of Cathode Spot

When a positive impulse of a relatively low voltage (V_s) is applied to the electrodes in a normal arrangement, the PS barely reaches the cathode, and the brightness of the PS is so weak that the PS arrival at the cathode can not be recognized on a still photograph, though it can be seen by the naked eye (Fig. 11(a)). In this case, the current pulse has a steep step-up front and a slowly decreasing tale slope. With an increasing V_s (Fig. 11(b)), the PS becomes brighter and the formation of a bright spot on the plane can been seen clearly, as shown in the photograph.[1],[2] At this instance, on the tale side of the current pulse, a small peak[21] is superimposed. A further increase of V_s makes bright spots on the plane and makes the channel bright in the mid gap space, while the second peak of the current approaches the wave front on an oscillogram and its magnitude increases (Fig. 11(c)). The light pulse was measured by the fixed slits of PM1 and PM2 at the rod tip $(x=0)$ and plane $(x=\delta)$ respectively. The time difference between
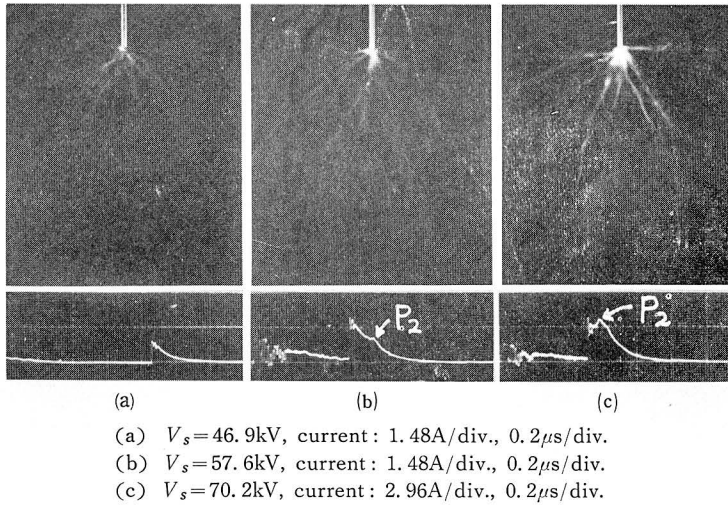
(a) $V_s = 46.9$ kV, current: 1.48A/div., 0.2μs/div.
(b) $V_s = 57.6$ kV, current: 1.48A/div., 0.2μs/div.
(c) $V_s = 70.2$ kV, current: 2.96A/div., 0.2μs/div.

Fig. 11. Variation of positive PS picture and current for different V_s.
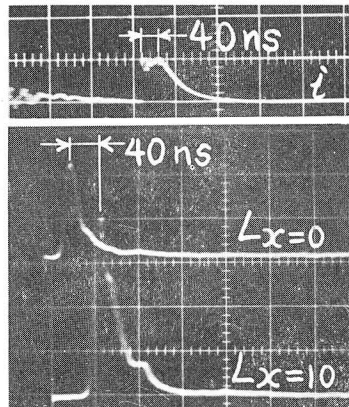$\rho = 2$ mm, $\delta = 10$ cm, normal arrangement, rod positive.

Fig. 12. Comparison between current and light pulse. $\rho = 2$ mm, $\delta = 10$ cm,
normal arrangement, rod positive, $V_p = 76.0$ kV. current: 1.48
A/div., 0.2 μs/div., light: 0.1 μs/div.

the 2 peaks in the current pulse and the time difference between the output pulses
of PM1 and PM2 i.e. the time for the PS arrival at the plane were found to be
almost identical (Fig. 12). Further, when the same voltage is applied to the gap
similar to that shown in Fig. 11(c), the light pulse at $x = \delta$ is formed by one, two,
or three peaks (due to several PS arrivals at the cathode at different times), and it
shows that under this experimental condition, cathode spots do not continue.

4. Characteristics of a Secondary Streamer

4.1 Special Features Observed from Photographs and The Light Pulse

⟨4.1.1⟩ Positive Polarity

Fig. 13 shows pictures of streamers where a positive impulse is applied to the gap ($\rho=2$mm, $\delta=5$ cm). In the region between the rod surface and the point where several mm away from the rod electrode, the bright discharge channel can be observed. The light pulse at this region, for example, $L_{x=0}$ (Fig. 13), has a sharp peak followed by a moderate second peak. This bright channel is the secondary streamer (abbreviated as SS in the following) named by Hudson et al.[1] Fig. 14 shows the variations of the SS as the applied voltage is changed. From these pictures, it is deduced that, for the same gap, the higher the voltage at the instance of the PS appearance
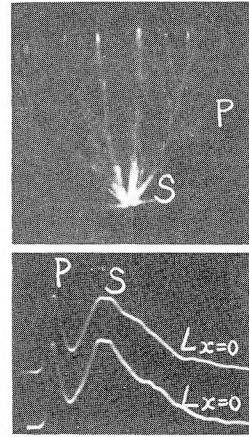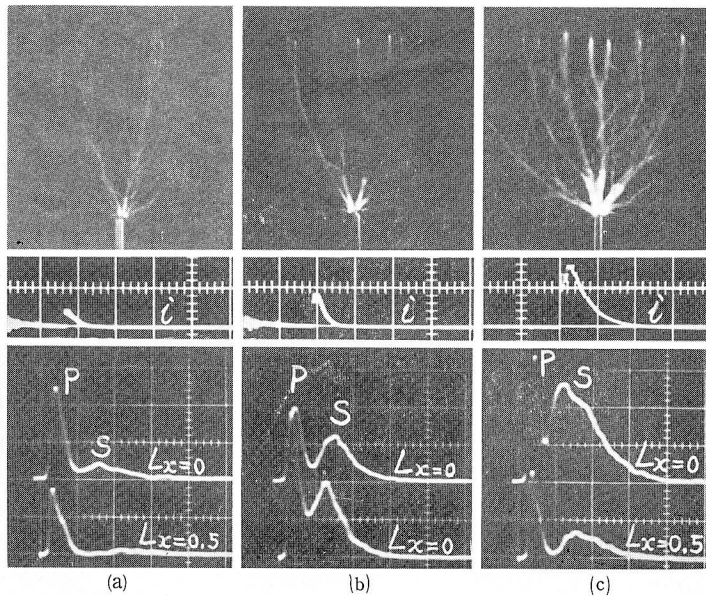

Fig. 13. Still photograph and light pulse for SS. $\rho=2$mm, $\delta=5$ cm, reversed arrangement, rod positive, $V_p=48.3$ kV. sweep: 50ns/div.

(a)   (b)   (c)

(a) $V_p=34.5$kV, current: 1.48A/div., 0.5μs/div., light: 0.1μs/div.
(b) $V_p=41.4$kV, current: 1.48A/div., 0.5μs/div., light: 0.1μs/div.
(c) $V_p=48.3$kV, current: 1.48A/div., 0.2μs/div., light: 0.1μs/div.

Fig. 14. Variation of SS for different applied voltage V_p. $\rho=2$mm, $\delta=5$cm, reversed arrangement, rod positive.
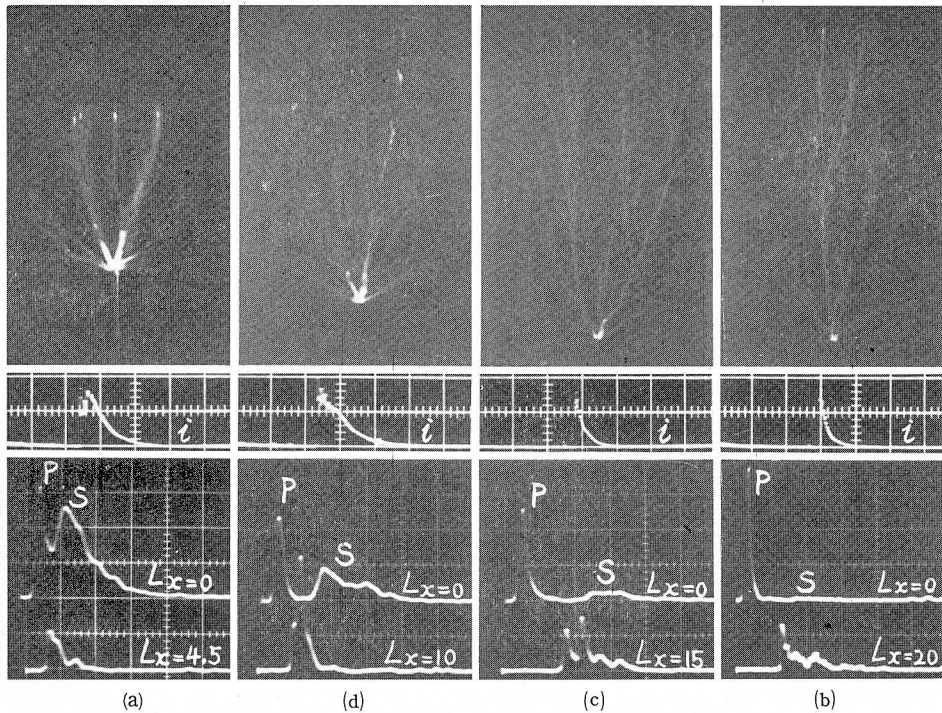
(a) $\delta=5$cm, $V_p=48.3$kV, current: 1.48A/div., 0.2μs/div., light: 0.1μs/div.
(b) $\delta=10$cm, $V_p=75.9$kV, current: 1.48A/div., 0.2μs/div., light: 0.1μs/div.
(c) $\delta=15$cm, $V_p=104$kV, current: 1.48A/div., 0.5μs/div., light: 0.1μs/div.
(d) $\delta=20$cm, $V_p=131$kV, current: 1.48A/div., 0.5μs/div., light: 0.2μs/div.

Fig. 15. Variation of SS for the change of δ. $\rho=2$mm, reversed arrangement,
rod positive, applying 10% FO voltage.

(V_s) is, the greater the SS brightness becomes. Further, the variations of the SS with
δ (5~20cm) are shown in Fig. 15. In each case, the applied voltage is near the
minimum FO voltage (10% FO voltage). From both the photograph and light pulse
oscillogram, it can be observed that the SS becomes more distinct as δ becomes smaller.
The common feature of streamers in both Fig. 14 and 15 is that the higher the aver-
age field intensity is, the more conspicuous the SS is. From the oscillogram of the
streamer current, there is no pulse in the current wave form which corresponds to
the light pulses of the SS.

⟨4.1.2⟩ Negative Polarity

In the case of a positive voltage application, the SS always propagates from the
rod electrode and can be distinguished easily. However it is different for the nega-
tive polarity, as can be seen in Fig. 16. In the case where the PS reaches the plane
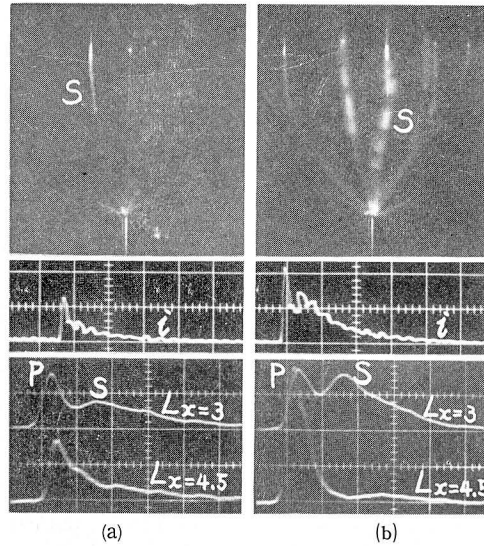
(a) Case of low V_s.   (b) Case of high V_s.

Fig. 16. Negative SS for different V_s. $\rho = 2$mm, $\delta = 5$cm, reversed arrangement, $V_p = 82.8$kV, current: 2.47A/div., 50ns/div., light: 50ns/div.

(Fig. 16(a)), the light pulse form $L_{x=3}$ has two peaks and is similar to the light pulse form $L_{x=0}$ (at the rod tip) in the case of the positive polarity. In addition, the streamer picture at $x = 3 \sim 5$ cm on the photograph shows an increase of brightness in the streamer channel. This may be considered as the negative SS corresponding to the positive SS. On the plane, a bright spot similar to that on the negative electrode found in the positive polarity case is observed, but it does not develop with time and hence is different from that spot on the cathode. In Fig. 16(b), for high V_s, the SS existence can be seen very clearly. Hence, it is deduced that the special feature of negative polarity is the numerous bright spots appearing along the discharge channel of the PS. These bright spots are found on the PS channel; and the light pulse due to these bright spots consists of 2 peaks (refer to $L_{x=3}$ in Fig. 16(b)) indicating that the second peak is due to the emission of the SS. Hence the bright spots on the channel reported[4] can be considered as those of the SS.

4.2 The Process from Secondary Streamer to Flashover

For a short gap, bridging the gap by a SS generates a PS, a SS and a Main stroke (arc)[1]−[3] successively. Hitherto, it has been reported that in a non-uniform field experiment, a PM tube,[1]−[3] and in a uniform field experiment, a Kerr cell camera[7],[8] or an image converter camera[23],[24] were used for the observation. In this

paper, however, by means of chopping the applied voltage, the breakdown process of a short gap subjected to a non-uniform field was recorded by still-photographs. The test gap used is made up of a conical electrode and a plane ($\rho=0.5$ mm, $\delta=3$ cm) in a normal arrangement. The applied voltage V_p has a maximum value of 80kV.

⟨4.2.1⟩ Positive Polarity

The experimental result obtained is shown in Fig. 17. The 50% FO voltage is 47kV and the rate of over voltage Δ is 70%. Firstly, the PS propagates from the anode (Fig. 17(a)). The chopping off time T_c is 12ns which is the time when the PS just reaches the plane with an average velocity of 2.5×10^8cm/s. At the point where the PS strikes upon the plane, the cathode spot occurs as shown in Fig. 17(c). Later, from the anode side, the SS begins to develop (Fig. 17(d)) and continues to propagate (Fig. 17(e)), finally reaching the plane after a time of $T_c=36$ns (Fig. 17(f)). The average propagating velocity of the SS is 1.5×10^8cm/s, and the discharge channel increases its luminosity with time. This state continues until $T_c=70$ns. When $T_c=80$ns, the discharge channel of the SS begins to transform into an arc channel, and the arc channel develops almost simultaneously from both the anode and the cathode (Fig. 17(g)). Each propagates into the gap, though the arc from the anode prop-
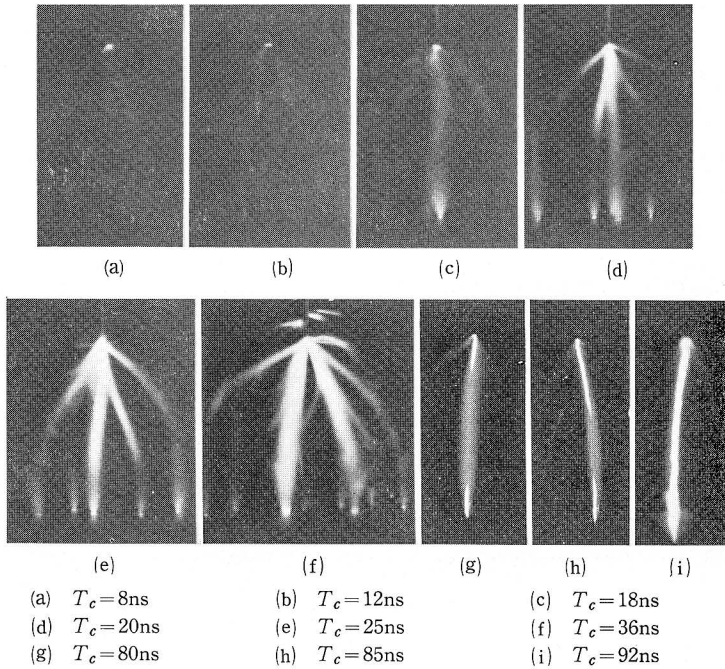

(a)	(b)	(c)	(d)

(e)	(f)	(g)	(h)	(i)

(a) $T_c=8$ns	(b) $T_c=12$ns	(c) $T_c=18$ns
(d) $T_c=20$ns	(e) $T_c=25$ns	(f) $T_c=36$ns
(g) $T_c=80$ns	(h) $T_c=85$ns	(i) $T_c=92$ns

Fig. 17. Flashover when positive SS bridges over the gap. Conical-to-plane gap, $\rho=0.5$mm, $\delta=3$cm, normal arrangement, $V_p=80$kV.

agates faster than that from the cathode (Fig. 17(h)). This arc has about a 0.3~0.6 mm diameter and is sharp at its tip. The arc takes 10ns to bridgeover the gap, and the breakdown completes after this stage (Fig. 17(i)). The current increases until it reaches a limiting value restricted by an external circuit.

⟨4.2.2⟩ **Negative Polarity**

The experimental results obtained are shown in Fig. 18. The 50% FO voltage is 61kV and V_p=80kV, which is equivalent to Δ=30%. Firstly, the PS develops from the cathode (Fig. 18(a)). The PS brightness around the cathode is slightly higher than the other parts which are darker compared with the case of positive polarity. Since the PS takes 19ns to reach the plane from the rod electrode, the average propagating velocity is 1.6×10^8cm/s. In addition, near the plane, the PS brightness increases to some extent. The longer the T_c is, the brighter is the whole discharge channel of the PS (Fig. 18(c)). Similarly, in the case of positive polarity, apparently the bright streamer propagates from the conical electrode, but it is not so distinct in the case of positive polarity. From the photograph, the brightness of the streamer channel increases uniformly. However, the region several mm away from the plane is slightly dark (Fig. 18(d)). Such a state continues until T_c=40ns (Fig. 18(e)).

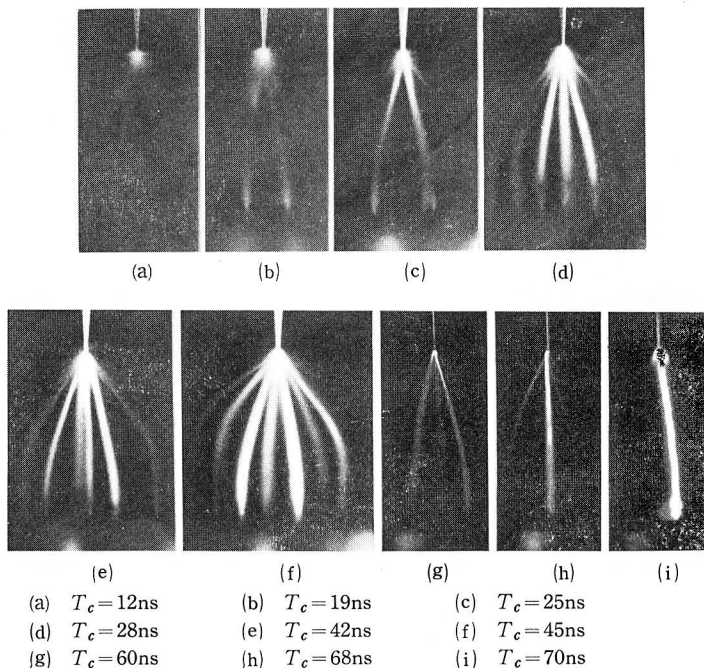(a)   (b)   (c)   (d)

(e)   (f)   (g)   (h)   (i)

(a) T_c=12ns	(b) T_c=19ns	(c) T_c=25ns
(d) T_c=28ns	(e) T_c=42ns	(f) T_c=45ns
(g) T_c=60ns	(h) T_c=68ns	(i) T_c=70ns

Fig. 18. Flashover when negative SS bridges over the gap. Conical-to-plane gap, ρ=0.5mm, δ=3cm, normal arrangement, V_p=80kV.

After that, the dark region disappears (Fig. 18(f)) and the discharge channel becomes increasingly brighter. Such phenomena are due to the field effects which keep the PS discharge channel bright and finally bring about the SS stage of the streamer. On the plane, a small bright spot can be observed, but it does not develop and has no important effect as has the cathode spot. For $T_c \fallingdotseq 60$ns, the arc channel begins to take place (Fig. 18(g)). Different from the positive polarity case, the arc starts from the cathode side only. After that, the arc develops into the gap space, but there is no arc formation from the anode side (Fig. 18(h)). The diameter of the arc develops to a magnitude of 0.5 mm, which is larger than that in the positive polarity case. Further, the arc tip is not pointed but diffusing outward. It takes 10ns for the arc to bridge over the gap (Fig. 18(i)), and the developing velocity is 3×10^8 cm/s.

As described above, in the breakdown phenomena of the short gap for the impulse voltage, a PS, a SS and an arc occur successively. The PS and SS channels are diverging by nature, while the arc channel is converging. A further comparison between the positive and negative polarity shows that the number of PS in the former is much larger, and the PS branching can observed. The spreading of the PS zone is wider than in the case of negative polarity.

4.3 Field Intensity of the Secondary Streamer

The SS occurrence is always accompanied by a PS and is due to some role played by the electric field. In the previous section, the authors thought the SS formation was due to the field effects along the PS channel. In this section, therefore, by measuring the field intensity within the SS channel, this thought is checked.

Against a positive voltage application to the gap, the SS occurs from the anode while against a negative voltage, the discontinuity along the discharge channel is observed. Hence, it is not appropriate to measure the SS length in the negative case. As a result, in this study, since the electric field of the SS can be obtained by measuring its length and the voltage difference, a reverse arrangement of the gap ($\rho=2$mm, $\delta=3$cm) was used for the positive polarity experiment. A voltage under FO voltage was used as a full wave, while a higher voltage than this was chopped off. In order to eliminate the effect of the applied voltage change during the PS development, the data of occurring the PS during the voltage wave front were discarded and only the data during the wave tale were adopted. Further, the data for the time shorter than 300ns between the PS occurrence and the chopping off were also discarded. In the case where Δ exceeds 25%, in order to satisfy these conditions, a steep-front impulse voltage was used. The results obtained are shown in Fig. 19. The characteristic of V_s vs. l is almost linear. Hence, by simple extrapolation, V_s becomes 61.5kV
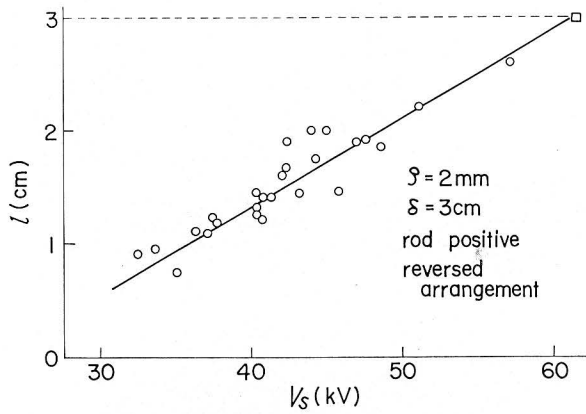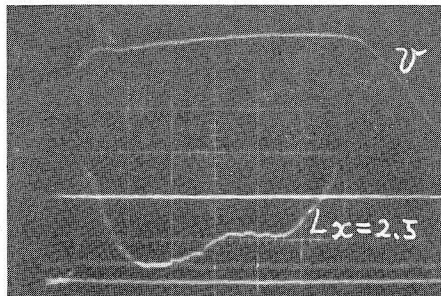
Fig. 19. V_s–l characteristics for positive SS.

Fig. 20. Voltage and light pulse form caused by flashover
occurrence. $\rho = 2$mm, $\delta = 3$cm, reversed arrange-
ment, rod positive. $V_p = 69.0$kV, sweep: 50ns/div.

when $l = 3$cm. Assuming the field to be constant along the SS channel, the value of
20.5 kV/cm can be obtained. This value coincides well with the voltage gradient of the
transient glow obtained by Meyer et al..[25] Fig. 20 shows a typical set of voltage and
light pulses when the SS reaches the plane and FO occurs. After the light pulse
corresponding to the PS is observed, the successive light pulse intensity (at a posi
tion 5 mm from the plane) remains almost at a constant level, and increases again
at the FO stage, while the corresponding voltage decreases rapidly. If the applied
voltage is chopped off at this stage of the constant light intensity, the result as shown
in Fig. 21(a) was obtained. In this figure, the symbol G represents the cathode spot
and the situation produced by the SS arrival at the cathode. Fig. 21(b) shows a
pulseless corona generated by applying negative DC voltage. Both are similar to each
other. Since the pulseless corona is a kind of glow discharge,[26] the region G is
probably a part of the glow also. Further, in Fig. 21(a), the region G and the SS

(a)   (b)
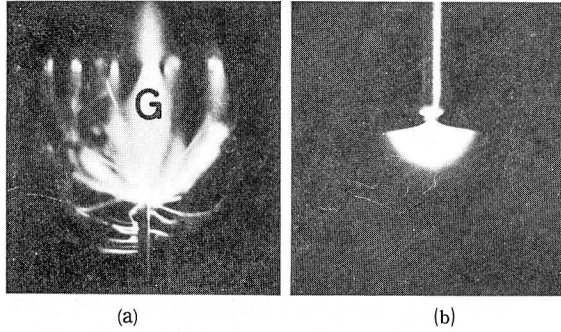
(a) SS. $\rho=2$mm, $\delta=3$cm, reversed arrangement, rod
      positive, $V_p=69.0$kV.
(b) Pulseless corona. $\rho=3$mm, $\delta=5$cm normal arrange-
      ment, rod negative, $V_{dc}=60$kV.
Fig. 21. Comparison between SS arrived at plane (under chopped
      voltage) and pulseless corona under DC voltage.

are smoothly joined to one another, without any discrete boundary. This is probably
because both have a similar property. Assuming the number of SS to be 3 and each
of them to have a 4 mm diameter, the current density J becomes 5.3 A/cm^2 when
the total current is 2A. Though the drift velocity of the electron at the field intensity
of 20 kV/cm is about 10^{6}cm/s, the electron density n in the SS channel becomes
3.3×10^{13}/cm^3. This value is lower than that of the arc channel by the order of 10^3
and corresponds to that of the glow.[28] Since the field of the SS is about 20 kV/cm
and $\alpha\approx\eta$[27] (where α and η are ionization and attachment coefficients respectively),
the ionization is capable of supplying the loss of charged particles within the chan
nel. Thus, from these data, it can be said that owing to the effect of the field along
the PS discharge channel, the portion emitting continuous light changes into the SS.

5. Conclusion

In this study, the pre-discharge phenomena for a rod-plane gap were investigat-
ed experimentally, and the characteristics of primary and secondary streamers were
deduced as follows :
(1) Before a breakdown occurs, the field intensity within the primary streamer
channel is 4.1~4.8 kV/cm for the positive polarity and 8.6~10.3 kV/cm for the
negative polarity, which is twice as much as in the former.
(2) For a negative voltage application, 6~7 times more energy than a positive
polarity case is necessary for the development of a primary streamer.
(3) In the PS discharge channel, the number of charged particles per cm is 3~4
$\times10^{10}$ in the positive polarity case, while 9~13$\times10^{10}$/cm in the negative polarity
case. The density of charged particles is 1~5$\times10^{12}$ and 3~16$\times10^{12}$cm^{-3} for the

positive and negative polarity case respectively.

(4) In the cases of both the positive and negative polarity, the secondary streame has identical paths as the primary streamer. In the positive polarity case, the SS develops from the anode towards the cathode, while in the negative polarity case, bright spots occur on the anode, cathode and along the PS channels.

(5) In the case of a bridgeover by the secondary streamer, for the positive polarity, the arc develops from both the anode and the cathode, while for the negative polarity, the arc develops only from the cathode.

(6) The field within the secondary streamer is about 20 kV/cm. This value implies the value of possible ionization by the electrical field.

(7) When a secondary streamer reaches the cathode, a glow discharge can be observed at the cathode. This glow has a smooth connection with the channel of the secondary streamer and it is not possible to distinguish it on the photographs.

Reference

1) Hudson, G. G., Loeb, L. B.: Phys. Rev. **123** (1961) 29
2) Dawson, G. A.: J. Appl. Phys. **36** (1965) 3391
3) Acker, F. E., Penney, G. W.: J. Appl. Phys. **39** (1968) 2363
4) Park, J. H., Cones, H. N.: J. R. N. B. S. **56** (1956) 201
5) Akazaki, M., Hara, M., Soma, K.: Trans. I. E. E. Japan **92**-A (1972) 553
6) Saxe, J. H., Meek, J. M.: P. I. E. E. **102**-c (1955) 221
7) Dunnington, F. G.: Phys. Rev. **38** (1931) 1535
8) White, H. J.: Phys. Rev. **46** (1934) 99
9) Loeb, L. B.: Electrical Coronas Chap. 3
10) Nasser, E., Loeb, L. B.: J. Appl. Phys. **34** (1963) 3340
11) Kritzinger, J. J.: Nature **197** (1963) 1165
12) Kritzinger, J. J.: Proc. 6th Intern. Conf. Ionization Phenomena of Gases, Paris (1963) paper VbII, p 295
13) Stekol'nikov, I. S., Shkilev, A. V.: Soviet Phys-Doklady **8** (1964) 825
14) Suzuki, T.: J. Appl. Phys. **42** (1971) 3766
15) Nishimaki, M.: Micro-wave Vacuume Tube and its Circuit, OHM-sha (1961)
16) Loeb, L. B.: Phys. Rev. **94** (1954) 227
17) I. E. E. Japan: Handbook of Discharge Phenomena, OHM-sha (1974) p 187
18) Suzuki, T.: J. Appl. Phys. **44** (1973) 4534
19) Nasser, E.: J. Appl. Phys. **42** (1971) 2839
20) Tsuneyasu, I., Akazaki, M.: Trans. I. E. E. Japan **93**-A (1973) 487
21) Isa, H.: Convention Record of I. E. E. Japan (1974) No. 69
22) Ikuta, N., Ushita, T., Ishiguro, Y.: J. I. E. E. Japan **90** (1970) 1816
23) Doran, A. A., Meyer, J.: Brit. J. Appl. Phys. **18** (1967) 793
24) Kekez, M. M., Barrault, M. R., Craggs, J. D.: J. Phys. D: Appl. Phys. **3** (1970) 1886

25)   Meyer, J., Lee, C. S.: J. Phys. D: Appl. Phys. 4 (1971) 168
26)   Sakai, O., Hosokawa, T., Miyoshi, Y. : J. I. E. E. Japan 78 (1958) 1413
27)   Harrison, M. A., Geballe, R.: Phys. Rev. 91 (1953) 1
28)   I. E. E. Japan : Handbook of Discharge Phenomena, OHM-sha (1974) p 140